opment. *Annu. Rev. Cell Dev. Biol.* **14,** 59–88
5. Bienz, M., and Clevers, H. (2000) Linking colorectal cancer to Wnt signaling. *Cell* **103,** 311–320
6. Gumbiner, B. M. (1997) Carcinogenesis: a balance between β-catenin and APC. *Curr. Biol.* **7,** R443–R446
7. Miller, J. R., and Moon, R. T. (1997) Analysis of the signaling activities of localization mutants of β-catenin during axis specification in *Xenopus*. *J. Cell Biol.* **139,** 229–243
8. Carnac, G., Kodjabachian, L., Gurdon, J. B., and Lemaire, P. (1996) The homeobox gene *Siamois* is a target of the Wnt dorsalisation pathway and triggers organiser activity in the absence of mesoderm. *Development* **122,** 3055–3065
9. Funayama, N., Fagotto, F., McCrea, P., and Gumbiner, B. M. (1995) Embryonic axis induction by the armadillo repeat domain of β-catenin: evidence for intracellular signaling. *J. Cell Biol.* **128,** 959–968
10. Glinka, A., Delius, H., Blumenstock, C., and Niehrs, C. (1996) Combinatorial signalling by Xwnt-11 and Xnr3 in the organizer epithelium. *Mech. Dev.* **60,** 221–231
11. Laurent, M. N., Blitz, I. L., Hashimoto, C., Rothbächer, U., and Cho, K. W. (1997) The *Xenopus* homeobox gene twin mediates Wnt induction of goosecoid in establishment of Spemann's organizer. *Development* **124,** 4905–4916
12. Sokol, S., Christian, J. L., Moon, R. T., and Melton, D. A. (1991) Injected Wnt RNA induces a complete body axis in *Xenopus* embryos. *Cell* **67,** 741–752
13. Sokol, S. Y. (1996) Analysis of Dishevelled signalling pathways during *Xenopus* development. *Curr. Biol.* **6,** 1456–1467
14. Briggs, M. W., and Sacks, D. B. (2003) IQGAP proteins are integral components of cytoskeletal regulation. *EMBO Rep.* **4,** 571–574
15. Mateer, S. C., McDaniel, A. E., Nicolas, V., Habermacher, G. M., Lin, M. J., Cromer, D. A., King, M. E., and Bloom, G. S. (2002) The mechanism for regulation of the F-actin binding activity of IQGAP1 by calcium/calmodulin. *J. Biol. Chem.* **277,** 12324–12333
16. Roy, M., Li, Z., and Sacks, D. B. (2004) IQGAP1 binds ERK2 and modulates its activity. *J. Biol. Chem.* **279,** 17329–17337
17. Li, Z., and Sacks, D. B. (2003) Elucidation of the interaction of calmodulin with the IQ motifs of IQGAP1. *J. Biol. Chem.* **278,** 4347–4352
18. Weissbach, L., Bernards, A., and Herion, D. W. (1998) Binding of myosin essential light chain to the cytoskeleton-associated protein IQGAP1. *Biochem. Biophys. Res. Commun.* **251,** 269–276
19. Kuroda, S., Fukata, M., Kobayashi, K., Nakafuku, M., Nomura, N., Iwamatsu, A., and Kaibuchi, K. (1996) Identification of IQGAP as a putative target for the small GTPases, Cdc42 and Rac1. *J. Biol. Chem.* **271,** 23363–23367
20. Briggs, M. W., Li, Z., and Sacks, D. B. (2002) IQGAP1-mediated stimulation of transcriptional co-activation by β-catenin is modulated by calmodulin. *J. Biol. Chem.* **277,** 7453–7465
21. Kuroda, S., Fukata, M., Nakagawa, M., Fujii, K., Nakamura, T., Ookubo, T., Izawa, I., Nagase, T., Nomura, N., Tani, H., Shoji, I., Matsuura, Y., Yonehara, S., and Kaibuchi, K. (1998) Role of IQGAP1, a target of the small GTPases Cdc42 and Rac1, in regulation of E-cadherin-mediated cell-cell adhesion. *Science* **281,** 832–835
22. White, C. D., Erdemir, H. H., and Sacks, D.B. (2012) IQGAP1 and its binding proteins control diverse biological functions. *Cell. Signal.* **24,** 826–834
23. Hart, M. J., Callow, M. G., Souza, B., and Polakis, P. (1996) QGAP1, a calmodulin-binding protein with a rasGAP-related domain, is a potential effector for cdc42Hs. *EMBO J.* **15,** 2997–3005
24. Brown, M. D., and Sacks, D. B. (2006) IQGAP1 in cellular signaling: bridging the GAP. *Trends Cell Biol.* **16,** 242–249
25. Goto, T., Sato, A., Shimizu, M., Adachi, S., Satoh, K., Iemura, S., Natsume, T., and Shibuya, H. (2013) IQGAP1 functions as a modulator of disheveled nuclear localization in Wnt signaling. *PLoS One* **8,** e60865
26. Chook, Y. M., and Süel, K. E. (2011) Nuclear import by karyopherin-βs: recognition and inhibition. *Biochim. Biophys. Acta* **1813,** 1593–1606
27. Görlich, D., and Kutay, U. (1999) Transport between the cell nucleus and the cytoplasm. *Annu. Rev. Cell Dev. Biol.* **15,** 607–660
28. Harel, A., and Forbes, D. J. (2004) Importin β: conducting a much larger cellular symphony. *Mol. Cell* **16,** 319–330
29. Lee, S. J., Sekimoto, T., Yamashita, E., Nagoshi, E., Nakagawa, A., Imamoto, N., Yoshimura, M., Sakai, H., Chong, K. T., Tsukihara, T., and Yoneda, Y. (2003) The structure of importin-β bound to SREBP-2: nuclear import of a transcription factor. *Science* **302,** 1571–1575
30. Kalderon, D., Richardson, W. D., Markham, A. F., and Smith, A. E. (1984) Sequence requirements for nuclear location of simian virus 40 large-T antigen. *Nature* **311,** 33–38
31. Itoh, K., Brott, B. K., Bae, G. U., Ratcliffe, M. J., and Sokol, S. Y. (2005) Nuclear localization is required for Dishevelled function in Wnt/β-catenin signaling. *J. Biol.* **4,** 3
32. Shimizu, K., and Gurdon, J. B. (1999) A quantitative analysis of signal transduction from activin receptor to nucleus and its relevance to morphogen gradient interpretation. *Proc. Natl. Acad. Sci. U.S.A.* **96,** 6791–6796
33. Blythe, S. A., Reid, C. D., Kessler, D. S., and Klein, P. S. (2009) Chromatin immunoprecipitation in early *Xenopus laevis* embryos. *Dev. Dyn.* **238,** 1422–1432
34. Natsume, T., Yamauchi, Y., Nakayama, H., Shinkawa, T., Yanagida, M., Takahashi, N., and Isobe, T. (2002) A direct nanoflow liquid chromatography-tandem mass spectrometry system for interaction proteomics. *Anal. Chem.* **74,** 4725–4733
35. Gan, X. Q., Wang, J. Y., Xi, Y., Wu, Z. L., Li, Y. P., and Li, L. (2008) Nuclear Dvl, c-Jun, β-catenin, and TCF form a complex leading to stabilization of β-catenin-TCF interaction. *J. Cell Biol.* **180,** 1087–1100
36. Macara, I. G. (2001) Transport into and out of the nucleus. *Microbiol. Mol. Biol. Rev.* **65,** 570–594
37. Izaurralde, E., Kutay, U., von Kobbe, C., Mattaj, I. W., and Görlich, D. (1997) The asymmetric distribution of the constituents of the Ran system is essential for transport into and out of the nucleus. *EMBO J.* **16,** 6535–6547
38. Asally, M., and Yoneda, Y. (2005) β-Catenin can act as a nuclear import receptor for its partner transcription factor, lymphocyte enhancer factor-1 (lef-1). *Exp. Cell Res.* **308,** 357–363
39. Fagotto, F., Glück, U., and Gumbiner, B. M. (1998) Nuclear localization signal-independent and importin/karyopherin-independent nuclear import of β-catenin. *Curr. Biol.* **8,** 181–190
40. Yokoya, F., Imamoto, N., Tachibana, T., and Yoneda, Y. (1999) β-Catenin can be transported into the nucleus in a Ran-unassisted manner. *Mol. Biol. Cell* **10,** 1119–1131

Downloaded from http://www.jbc.org/ at TSUKUBA DAIGAKU on February 18, 2014

FEBS Letters 587 (2013) 3749–3754

FEBS Letters

journal homepage: www.FEBSLetters.org

# Mesdc2 plays a key role in cell-surface expression of Lrp4 and postsynaptic specialization in myotubes

Taisuke Hoshi [a], Tohru Tezuka [a], Kazumasa Yokoyama [a], Shun-ichiro Iemura [b], Tohru Natsume [c], Yuji Yamanashi [a,*]

[a] Division of Genetics, Department of Cancer Biology, The Institute of Medical Science, The University of Tokyo, Tokyo, Japan
[b] Translational Research Center, Fukushima Medical University, Fukushima, Japan
[c] Molecular Profiling Research Center for Drug Discovery, National Institute of Advanced Industrial Science and Technology, Tokyo, Japan

ARTICLE INFO

*Article history:*
Received 29 July 2013
Revised 24 September 2013
Accepted 3 October 2013
Available online 15 October 2013

Edited by Michael R. Bubb

*Keywords:*
Chaperon
Glycosylation
Lrp4
Neuromuscular junction

ABSTRACT

**Low-density lipoprotein receptor-related protein 4 (Lrp4) is essential for pre- and post-synaptic specialization at the neuromuscular junction (NMJ), an indispensable synapse between a motor nerve and skeletal muscle. Muscle-specific receptor tyrosine kinase MuSK must form a complex with Lrp4 to organize postsynaptic specialization at NMJs. Here, we show that the chaperon Mesdc2 binds to the intracellular form of Lrp4 and promotes its glycosylation and cell-surface expression. Furthermore, knockdown of Mesdc2 suppresses cell-surface expression of Lrp4, activation of MuSK, and postsynaptic specialization in muscle cells. These results suggest that Mesdc2 plays an essential role in NMJ formation by promoting Lrp4 maturation.**

*Structured summary of protein interactions:*
**Lrp4** physically interacts with **CANX**, **LRPAP1**, **CCAR2**, **MESDC2**, **PDIA4**, **RPN1** and **SDF2L1** by anti tag coimmunoprecipitation (View interaction)
**Mesdc2** physically interacts with **Lrp4** by anti tag coimmunoprecipitation (View interaction)
**Mesdc2** physically interacts with **Lrp4** by anti bait coimmunoprecipitation (View interaction)

**© 2013 Federation of European Biochemical Societies. Published by Elsevier B.V. All rights reserved.**

## 1. Introduction

The contraction of skeletal muscle is controlled by motor neurons, which contact the muscle fibers at the neuromuscular junction (NMJ), a synapse that uses the neurotransmitter acetylcholine (ACh) in mammals. For efficient neuromuscular transmission, ACh receptors (AChRs) must be densely clustered on the postsynaptic membrane at NMJ [1,2]. The formation of the NMJ is orchestrated by the muscle-specific receptor tyrosine kinase MuSK, which forms a complex with Lrp4, a member of the low-density lipoprotein receptor-related protein (Lrp) family [3–5]. Prior to motor nerve innervation, MuSK is activated in a manner dependent on its cytoplasmic activator Dok-7 together with Lrp4, and induces postsynaptic specialization including AChR clustering in the central region of muscle [4–7]. After innervation, neural agrin (hereafter referred to as "agrin"), a glycoprotein secreted from presynaptic nerve terminals, binds to Lrp4 and further upregulates MuSK's activity to establish the postsynaptic apparatus of the NMJ [4,5]. In addition, it was recently reported that Lrp4 interacts with the motor axon and acts as an important retrograde signal to induce presynaptic specialization [8,9]. Furthermore, we and others identified autoantibodies that recognize the extracellular region of Lrp4 in patients with myasthenia gravis, an autoimmune neuromuscular disease. These antibodies showed inhibitory effects on agrin's binding to the cell-surface receptor Lrp4 and subsequent clustering of AChRs on cultured myotubes, supporting an essential role for the agrin-Lrp4 axis in the maintenance of NMJs [10–12]. However, in contrast to the depth of our understanding of Lrp4 functions, it remains largely unknown how its function and subcellular localization are regulated.

In this study, we found that the chaperon protein Mesoderm development candidate 2 (Mesdc2) binds to Lrp4 and facilitates

*Abbreviations:* ACh, acetylcholine; AChR, ACh receptor; Btx, bungarotoxin; CMS, congenital myasthenic syndrome; Dok-7, downstream of tyrosine kinases 7; DPAGT1, dolichyl-phosphate (UDP-N-acetylglucosamine) N-acetylglucosamine-phosphotransferase 1; GFPT1, glutamine–fructose-6-phosphate transaminase 1; LC–MS/MS, liquid chromatography–tandem mass spectrometry; Lrp4, low-density lipoprotein receptor-related protein 4; Mesdc2, mesoderm development candidate 2; MuSK, muscle-specific kinase; NMJ, neuromuscular junction; TM, tunicamycin; WCL, whole cell lysates

* Corresponding author. Address: Division of Genetics, Department of Cancer Biology, The Institute of Medical Science, The University of Tokyo, 4-6-1 Shirokanedai, Minato-ku, Tokyo 108-8639, Japan. Fax: +81 3 6409 2116.
*E-mail address:* yyamanas@ims.u-tokyo.ac.jp (Y. Yamanashi).

0014-5793/$36.00 © 2013 Federation of European Biochemical Societies. Published by Elsevier B.V. All rights reserved.
http://dx.doi.org/10.1016/j.febslet.2013.10.001

its glycosylation. Moreover, Mesdc2 is a key regulator of cell-surface expression of Lrp4, activation of MuSK, and consequent postsynaptic specialization in cultured myotubes. Together, these findings suggest an important role for the chaperon in NMJ formation.

## 2. Materials and methods

### 2.1. Antibodies and a recombinant protein

Antibodies used in this study were obtained from the following resources: rabbit monoclonal anti-Lrp4 (Epitomics) and anti-Mesdc2 (C22F5, for immunoblotting, Cell Signaling); mouse monoclonal anti-Flag (1E6, for immunoprecipitation and immunoblotting, Wako; M2, for immunoblotting of immunoprecipitated Flag-Mesdc2, Sigma), anti-phosphotyrosine (4G10, Millipore), and anti-α-Tubulin (DM1A, Santa Cruz); goat polyclonal anti-Actin (I-19, Santa Cruz), anti-Mesdc2 (AF4545, for immunoprecipitation, R&D Systems), anti-MuSK (AF562, for immunoblotting, R&D Systems; N-19 and C-19, 1:1 mixture for immunoprecipitation, Santa Cruz), and control IgG (Santa Cruz); and rabbit polyclonal anti-AChR β1 (H-101, Santa Cruz) antibodies. The recombinant 90 kDa C-terminal fragment of neural agrin was obtained from R&D Systems.

### 2.2. Plasmids

The mouse Lrp4 expression plasmids were described previously [10]. The cDNA encoding Lrp4 with a Flag epitope at its C-terminus was generated by PCR, and cloned into the pcDNA3.1/myc-His plasmid (Invitrogen). The mouse Mesdc2 cDNA was cloned by RT-PCR from poly(A)$^+$ RNA from C2C12 myotubes. The cDNA encoding Mesdc2, in which a Flag epitope was inserted after the signal sequence, was generated by PCR, and cloned into pcDNA3.1/myc-His plasmid. The shRNA sequences for mouse Mesdc2 and the non-silencing control are as follows:

Mesdc2 shRNA#1 (target sequence): 5′-GCCTGTTGTATCTGTGTATTA-3′,

Mesdc2 shRNA#2 (target sequence): 5′-TTGTTCAGTGAGTGAA GATAA-3′,

Control shRNA (target sequence): 5′-TTCTCCGAACGTGTCACGT-3′.

These shRNA sequences were inserted into the pSIREN-RetroQ plasmid (Takara Bio).

### 2.3. Cell culture, transfection, tunicamycin treatment, and retrovirus infection

HEK293T and Plat-E Retroviral packaging cells were cultured in high glucose Dulbecco's Modified Eagle Medium (DMEM) supplemented with 10% FBS. C2C12 myoblasts were cultured in DMEM supplemented with 20% FBS. For differentiation into myotubes, myoblasts were grown to confluency, and fed with differentiation medium (DMEM supplemented with 2% horse serum) for 3–5 days. Expression plasmids were transfected using FuGENE6 (Roche) or Lipofectamine 2000 (for LC–MS/MS analysis, Invitrogen) according to the manufacturer's instruction. For liquid chromatography–tandem mass spectrometry (LC–MS/MS) analysis, HEK293T cells were transfected with the expression plasmids of Lrp4-Flag and incubated at 37 °C for 24 h. For tunicamycin (TM) treatment, HEK293T cells were transfected with expression plasmids and incubated at 37 °C overnight. The next day, the cells were incubated in the presence of TM for 16 h. For production of retrovirus, the pSIREN-RetroQ plasmids were transfected into Plat-E cells. Forty-eight hours after transfection, the culture medium were collected, filtrated through a 0.22 μm filter (Millipore), and administered to C2C12 myoblasts for infection. Eight hours after infection, the virus-containing culture medium was removed and the cells were fed with fresh medium and incubated at 37 °C overnight. The next day, puromycin was added to culture media at 1 μg/ml, and the cells were cultured for an additional 6 days to remove uninfected cells.

### 2.4. Digestion of Lrp4-binding proteins and LC–MS/MS analysis

HEK293T cells transfected with plasmids expressing Lrp4-Flag were solubilized in TNE buffer [13]. The lysates were incubated with mouse monoclonal anti-Flag antibody-conjugated agarose (M2, Sigma) at 4 °C for 1h and subjected to immunoprecipitation. Lrp4-Flag and co-precipitated proteins were eluted from the slurry with an excess of Flag peptides, digested with lysyl endopeptidase C (Wako), and analyzed with a highly sensitive direct nanoflow LC–MS/MS system as previously described [13,14].

### 2.5. Immunoblotting, immunoprecipitation, and α-bungarotoxin pull-down

Immunoblotting, immunoprecipitation, and α-bungarotoxin (α-Btx) pull-down were performed as described previously [7,15]. To examine phosphorylation of MuSK and AChR, C2C12 myotubes expressing shRNAs were treated with or without agrin (100pM) at 37 °C for 30 min prior to these assays.

### 2.6. Deglycosylation of Lrp4

The membrane fraction from HEK293T cells transfected with expression plasmids of Lrp4 was purified as previously described [15], and the fraction was denatured at 100 °C for 10 min in 1× denaturing buffer (NEB) before incubation with N-glycosidase F (for removal of Asn-linked glycans, NEB) and/or a mixture of Neuraminidase and O-glycosidase (for removal of Ser/Thr-linked glycans, NEB) at 37 °C for 3 h in 1× G7 reaction buffer (NEB) supplemented with 1% NP-40. Reactions were stopped by the addition of Laemmli sample buffer.

### 2.7. Biotinylation of cell-surface proteins

To label the cell-surface proteins with biotin, cells were washed with PBS and treated with EZ-link Sulfo-NHS-LC-Biotin (Pierce) (0.5 mg/ml PBS) at 4 °C for 30 min. The reaction was stopped by two consecutive 20 min treatments with 100 mM Glycine in PBS at 4 °C. NeutrAvidin Agarose Resin (Pierce) and Avidin-HRP (eBioscience) was used to pull down and detect the biotinylated cell-surface proteins, respectively, as described elsewhere [16,17].

### 2.8. AChR clustering assay

Myotubes were treated with or without agrin (10 pM) at 37 °C for 16 h, incubated with Alexa 594-conjugated α-Btx (Invitrogen) at 37 °C for 1 h, and fixed. Fluorescence images of fixed myotubes were collected with a DM6000B microscope (Leica), and the number of AChR clusters (>5 μm in their longest diameter) was counted, as described elsewhere [5,18].

### 2.9. Statistical analysis

All experiments were performed at least 3 times. The quantitative results were expressed as the means ± SEM. Statistical significance was determined by the paired $t$ test, unless otherwise noted.

## 3. Results

### 3.1. Mesdc2 binds to Lrp4

To gain insights into regulatory mechanisms controlling Lrp4-mediated signaling, we searched for Lrp4-binding proteins.

**Table 1**
Identification of Mesdc2 as a candidate Lrp4-binding protein by mass spectrometry. Molecular mass to charge ratio (*m*/*z*) and charge of each peptide ion observed in LC–MS/MS analysis together with the assigned amino acid sequence and its position in the corresponding human Mesdc2 protein are shown.

| Protein | Peptide (*m*/*z*) | Charge | Sequence | Residues (start–end) |
|---|---|---|---|---|
| Mesdc2 | 794.39 | 3 | DIRDYNDADMARLLEQWEK | 54–72 |
| | 504.55 | 3 | DDDIEEGDLPEHK | 73–85 |
| | 552.28 | 2 | RPSAPVDFSK | 86–95 |
| | 814.41 | 2 | TLMMFVTVSGSPTEK | 113–127 |

The Lrp4-Flag expression plasmids were introduced into HEK293T cells, and Lrp4-Flag together with its binding partners were immunoprecipitated with anti-Flag antibodies. The immunoprecipitates were digested and analyzed with a highly sensitive direct nanoflow LC–MS/MS system [13,14]. Following a database search, we identified peptides apparently derived from 7 candidate binding proteins (Supplementary Table 1), including four from Mesoderm development candidate 2 (Mesdc2) (Table 1). Because binding of overexpressed Mesdc2 to other Lrp-family proteins had been reported [19], we performed a similar test. We immunoprecipitated Flag-Mesdc2 from the lysates of HEK293T cells transfected with Lrp4 and Flag-Mesdc2 expression plasmids, and confirmed that Lrp4 was co-immunoprecipitated with Flag-Mesdc2 only when both proteins were expressed (Fig. 1A). Although anti-Lrp4 antibodies detected two discrete forms with apparent molecular masses of about 265 and 233 kDa (hereafter referred to as "upper Lrp4" and "lower Lrp4", respectively) (Fig. 1A), lower Lrp4 was selectively co-immunoprecipitated with Flag-Mesdc2 (Fig. 1B). Because cell-surface receptor proteins are generally glycosylated, we examined whether the glycosylation status differs between the two forms of Lrp4 [20]. The membrane fraction prepared from HEK293T cells expressing exogenous Lrp4 was treated with N-glycosidase F and/or a mixture of Neuraminidase and O-glycosidase. Removal of Ser/Thr-linked (O-linked) glycans with the latter mixture increased the mobility of upper but not lower Lrp4 (Fig. 1C). On the other hand, treatment with N-glycosidase F to remove Asn-lined (N-linked) glycans resulted in a mobility shift of both upper and lower Lrp4 (Fig. 1C). These data indicate that both forms of Lrp4 are N-glycosylated, and that upper Lrp4 is further O-glycosylated, aside from glycosylation undetectable in the assay, if any [21]. We still observed two forms of Lrp4 after removal of both N- and O-linked glycans, implying that upper Lrp4 has additional post-translational modification(s) (Fig. 1C), the nature of which is currently unknown. Taken together, these findings indicate that Mesdc2 binds to lower Lrp4, which appears to lack O-linked glycans.

### *3.2. Mesdc2 facilitates glycosylation and cell-surface expression of Lrp4*

Although Mesdc2 binds to lower Lrp4, forced expression of Mesdc2 appeared to increase upper Lrp4 (Fig. 1A). Therefore, we evaluated expression levels of upper Lrp4 upon forced expression of Mesdc2 in HEK293T cells and confirmed significantly elevated expression of upper Lrp4 (Fig. 2A), which is O-glycosylated unlike lower Lrp4 (Fig. 1C). Because receptor proteins synthesized and correctly folded in the endoplasmic reticulum are transported to the Golgi apparatus, where protein O-glycosylation takes place [22], our findings suggest that Mesdc2 may facilitate such glycosylation and trafficking of Lrp4 in the secretory pathway to the cell surface as a chaperon. Indeed, previous studies suggested a similar chaperon role for Mesdc2 with two Lrp4-related proteins, Lrp5 and Lrp6 [19,23]. To test if Mesdc2 chaperons Lrp4, we examined expression levels of Lrp4 on the cell-surface membrane by treating HEK293T cells with a membrane-impermeable biotinylation reagent to specifically label cell-surface proteins. Co-expression of Mesdc2 with Lrp4 significantly increased cell-surface levels of the latter (Fig. 2B), supporting a role for Mesdc2 in chaperoning Lrp4. We also found that upper Lrp4 corresponds to the cell-surface form with regard to apparent molecular mass, suggesting that upper Lrp4 is the mature, cell-surface form (Supplementary Fig. 1). Although we detected a very minor biotinylated form of Lrp4 with apparently lower molecular mass, it could be a degradation product of the upper, major, cell-surface form of Lrp4, or a differently modified form of it. A fuller understanding of its molecular nature awaits further studies.

N-linked glycosylation is usually important for appropriate folding of receptor proteins and subsequent modifications and transport to the cell surface [22,24]. To address its contribution to Lrp4 expression on the surface, we utilized tunicamycin (TM), a specific inhibitor of N-linked glycosylation [25]. TM treatment significantly suppressed cell-surface expression of Lrp4, suggesting that N-linked glycosylation of Lrp4 is essential for its trafficking to

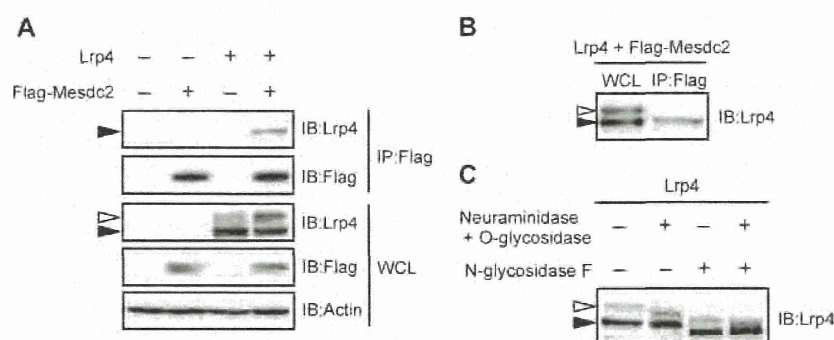


**Fig. 1.** Mesdc2 binds to Lrp4. (A and B) HEK293T cells were transfected with expression plasmids for Lrp4 and/or Flag-Mesdc2. Whole cell lysates (WCL) were subjected to immunoprecipitation (IP) with anti-Flag antibody. The immunoprecipitates and WCL were subjected to immunoblotting (IB) with the indicated antibodies. Positions of upper Lrp4 (▷) and lower Lrp4 (►) are shown. (C) Membrane fractions of HEK293T cells transfected with Lrp4 expression plasmids were treated with N-glycosidase F and/or a mixture of Neuraminidase and O-glycosidase. The mobility shift of Lrp4 by deglycosylation was analyzed by IB with anti-Lrp4 antibodies.

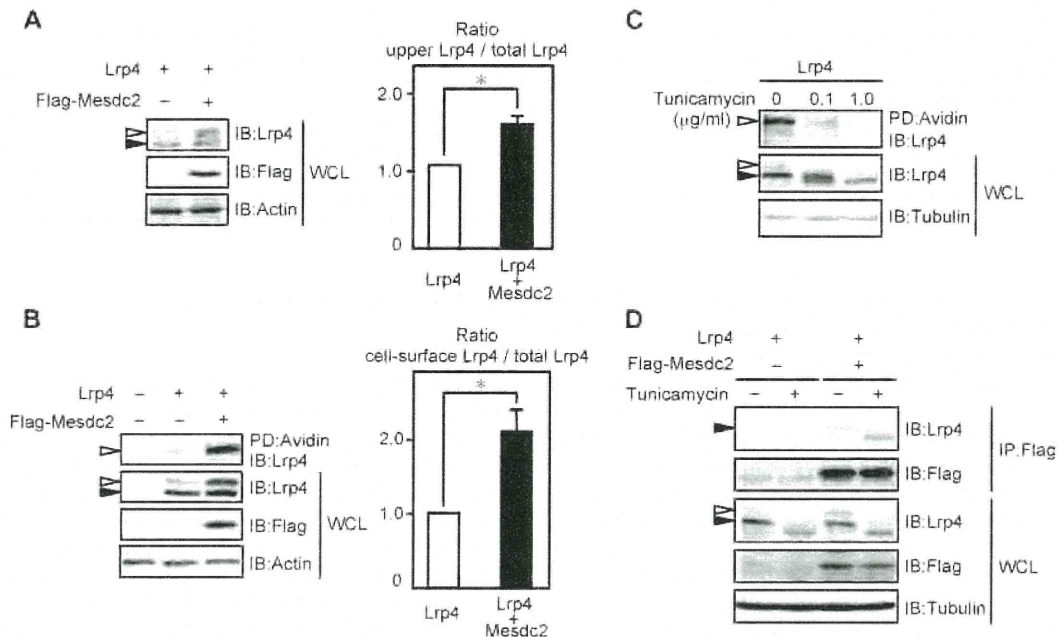


**Fig. 2.** Mesdc2 promotes glycosylation and cell-surface expression of Lrp4 in HEK293T cells. HEK293T cells were transfected with expression plasmids for Lrp4 and/or Flag-Mesdc2, and subjected to the following assays. (A) WCL were subjected to IB with the indicated antibodies (left). Positions of upper Lrp4 (▹) and lower Lrp4 (▸) are shown. Ratio of upper Lrp4 to total Lrp4 was quantified using a chemiluminescence imager (right). The ratio in cells transfected with Lrp4 plasmids alone is arbitrarily defined as 1.0. Data are expressed as means ± SEM from three independent experiments performed in triplicate. * Denotes $P < 0.05$. (B) Cell-surface expression of Lrp4 in transfected HEK293T cells was analyzed by the biotin-labeling-based quantification of cell-surface proteins. The biotinylated cell-surface proteins pulled down (PD) with NeutrAvidin Agarose and WCL were subjected to IB with the indicated antibodies (left). Ratio of cell-surface Lrp4 to total Lrp4 in HEK293T cells was quantified (right). The ratio in cells transfected with Lrp4 plasmids alone is arbitrarily defined as 1.0. Data are shown as means ± SEM. $n = 6$; $^{*}P < 0.05$. (C) Transfected HEK293T cells were treated with tunicamycin (0.1 or 1.0 μg/ml) for 16 h. The cell-surface expression of Lrp4 was analyzed as described above. (D) Transfected HEK293T cells were treated with tunicamycin (1.0 μg/ml) for 16 h and WCL were subjected to IP with anti-Flag antibody. The immunoprecipitates and WCL were subjected to IB with the indicated antibodies.

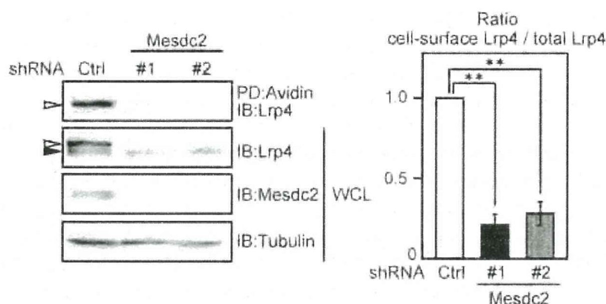


**Fig. 3.** Mesdc2 regulates cell-surface expression of Lrp4 in myotubes. Cell-surface expression of Lrp4 on the C2C12 myotubes expressing shRNAs against Mesdc2 (#1 and #2) or the control (Ctrl) was analyzed as in Fig. 2B (left). Positions of upper Lrp4 (▹) and lower Lrp4 (▸) are shown. Ratio of cell-surface Lrp4 to total Lrp4 was quantified (right). The ratio in cells expressing the control shRNA is arbitrarily defined as 1.0. Data are shown as means ± SEM. $n = 4$; $^{**}P < 0.01$.

the surface (Fig. 2C). It should be noted that binding of Mesdc2 to Lrp4 was not significantly affected by the presence of TM (Fig. 2D), indicating that N-glycosylation of Lrp4 is not a prerequisite for the binding to Mesdc2. Together, our findings suggest that Mesdc2 binds to the immature form of Lrp4 to promote its glycosylation and cell-surface expression.

### *3.3. Mesdc2 is a key regulator of cell-surface expression of Lrp4, MuSK activation, and postsynaptic specialization in muscle cells*

As mentioned above, the receptor tyrosine kinase MuSK must form a complex with Lrp4 to orchestrate postsynaptic specialization at NMJs on myotubes [4–6]. Thus, we examined if Mesdc2 plays a role in cell-surface expression of Lrp4, MuSK activation, and subsequent postsynaptic specialization in cultured myotubes. To confirm binding of Mesdc2 to lower Lrp4 in these cells, we performed a co-immunoprecipitation assay with myotubes differentiated from C2C12 myoblasts and detected lower Lrp4 in anti-Mesdc2 immunoprecipitates (Supplementary Fig. 2). Thus, we designed two non-overlapping shRNA sequences against Mesdc2, and introduced them into C2C12 myoblasts using a retroviral vector. Infected myoblasts were selected as described in Materials and methods and differentiated into myotubes, and cell-surface expression of Lrp4 was evaluated as mentioned. We confirmed reduced expression of Mesdc2, which strongly inhibited cell-surface expression of Lrp4 (Fig. 3). Mesdc2 downregulation also reduced expression levels of upper Lrp4, supporting the idea that it is the mature, cell-surface form of Lrp4. Next, we tested whether reduction of Mesdc2 inhibits MuSK activation and subsequent AChR clustering, both of which are dependent on Lrp4 in myotubes [4,5]. Indeed, knockdown of Mesdc2 impaired agrin-induced activation of MuSK, as judged by its autophosphorylation, although MuSK's phosphorylation was undetectable in the absence of agrin irrespectively of the knockdown (Fig. 4A). Moreover, tyrosine phosphorylation of AChR, which is triggered on activation of MuSK [26], was significantly suppressed by the downregulation either in the presence or absence of agrin (Fig. 4B). However, cell-surface expression of MuSK was not significantly affected by the knockdown of Mesdc2 (Supplementary Fig. 3A). These results indicate that Mesdc2 plays an essential role in MuSK activation together with glycosylation and cell-surface expression of Lrp4 in myotubes. Consistently, downregulation of Mesdc2 suppressed AChR clustering, a characteristic event of MuSK-dependent postsynaptic specialization, in myotubes (Fig. 4C), although it did not significantly affect cell-surface expression of AChR (Supplementary Fig. 3B). Together, these findings demonstrate that the chaperon protein Mesdc2 plays a key role in MuSK-dependent postsynaptic

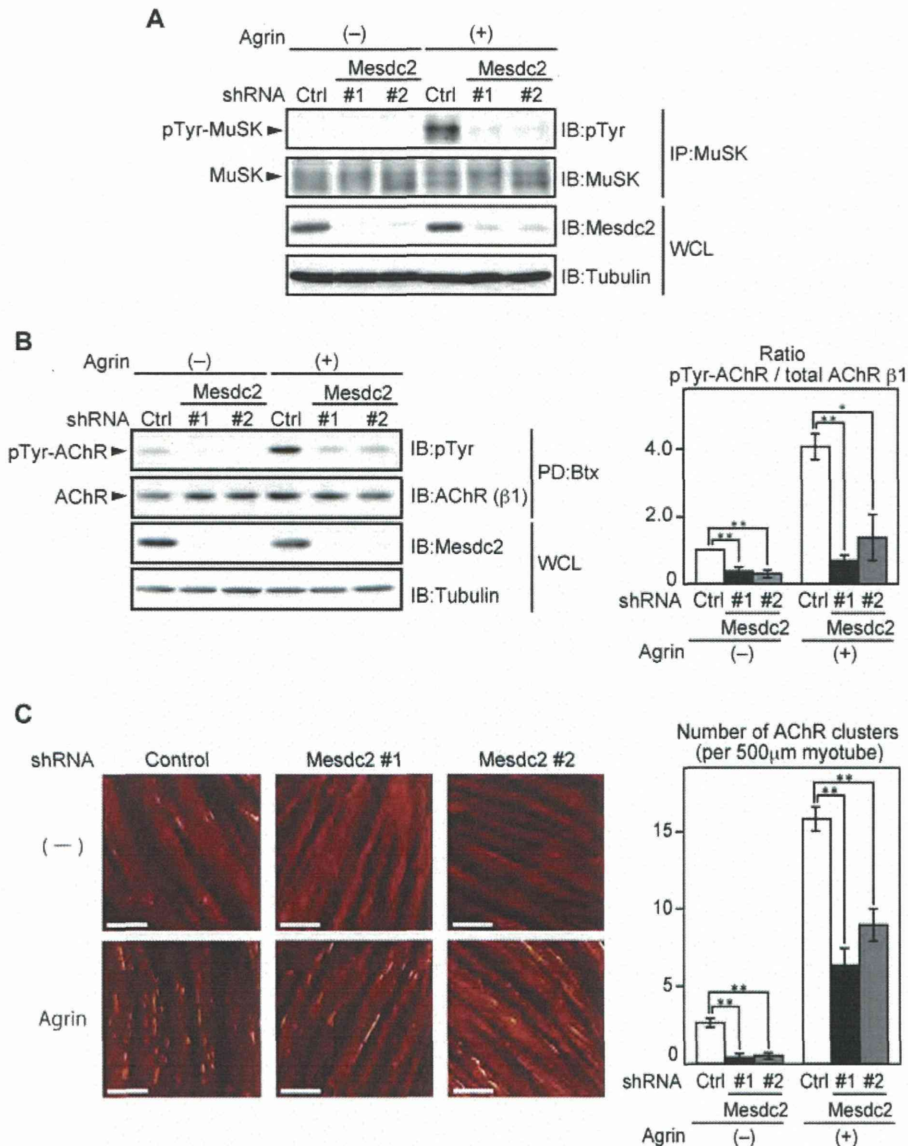


**Fig. 4.** Mesdc2 regulates MuSK activation and AChR clustering in myotubes. C2C12 myotubes expressing the indicated shRNAs were treated with or without agrin. (A) WCL were subjected to IP with anti-MuSK antibodies. The immunoprecipitates and WCL were subjected to IB with the indicated antibodies. pTyr denotes phosphotyrosine. Positions of MuSK and its tyrosine-phosphorylated form are shown. (B) WCL were incubated with α-Bungarotoxin (α-Btx)-conjugated sepharose to pull down AChR. The precipitates and WCL were subjected to IB with the indicated antibodies (left). Positions of AChR (β1 subunit) and its tyrosine-phosphorylated form are shown. Ratio of tyrosine phosphorylated AChR to total AChR β1 was quantified (right). The ratio in untreated cells expressing the control shRNA is arbitrarily defined as 1.0. Data are shown as means ± SEM. $n \geqslant 5$; $^{*}P < 0.05$, $^{**}P < 0.01$. (C) Myotubes were stained with Alexa594-conjugated α-Btx to visualize AChR clusters (left). Scale bar, 100 μm. The numbers of AChR clusters per 500 μm myotube length interval ($n \geqslant 20$) were counted (right). Data are expressed as means ± SEM of the numbers from three or more independent experiments. Statistical significance was determined using a Student's $t$-test ($^{**}P < 0.01$).

specialization probably by promoting glycosylation and cell-surface expression of Lrp4 in myotubes.

## 4. Discussion

In the present study, we demonstrated that Mesdc2 positively regulates cell-surface expression of Lrp4 and postsynaptic specialization in cultured myotubes. Lrp4 forms a complex with MuSK, binds to motor neuron-derived agrin, and stimulates MuSK's kinase activity in cooperation with muscle cytoplasmic protein Dok-7 [4,5,7]. In addition, Lrp4 binds to the motor axon and induces presynaptic specialization [8,9]. To exert these activities essential for neuromuscular synaptogenesis, Lrp4 must be expressed on the cell-surface membrane of myotubes. Therefore, our findings suggest that Mesdc2 plays a critical role in NMJ formation by promoting cell-surface expression of Lrp4. We revealed that Mesdc2 binds to the less glycosylated, intracellular form of Lrp4 but not the mature, cell-surface form (Fig. 1B). We also found that inhibition of N-linked glycosylation prevents cell-surface expression of Lrp4, but not Lrp4-Mesdc2 binding (Fig. 2C and D). These findings suggest that cell-surface expression of Lrp4 requires both Mesdc2-mediated chaperoning and N-linked glycosylation. This type of glycosylation plays an important role in the association between several glycoproteins and the lectin chaperons Calnexin and Calreticulin, which is important for appropriate folding of their target proteins [20,22]. Because Calnexin was identified as one of the potential binding partners of Lrp4 by our LC-MS/MS analysis (Supplementary Table 1), this lectin chaperon may also

facilitate correct folding of Lrp4. Although it remains unclear how Mesdc2 regulates cell-surface expression of Lrp4, it was reported that Mesdc2 prevents protein aggregation and improper disulfide-bond formation of Lrp6 [19]. Similar mechanisms may underlie Mesdc2-mediated regulation of Lrp4.

In addition to Lrp4, many key NMJ proteins are known to undergo glycosylation that regulates their activities [27]. For example, N-linked glycosylation of AChR subunits is required for their correct folding and cell-surface expression [28]. Recently *GFPT1* and *DPAGT1*, two genes encoding key enzymes for synthesis of an important building block of N-glycans, were identified as the causative genes for certain types of congenital myasthenic syndromes (CMSs), a group of inherited NMJ disorders [25,29]. Patients with either *GFPT1* or *DPAGT1* mutations showed reduced expression of AChRs in the endplate, which is a region of postsynatic specialization on myotubes, suggesting that AChR subunits and/or regulators of their expression at NMJs are critical targets of these N-glycosylation-related enzymes. Given that MuSK activation induces expression of AChR subunits [30,31], N-glycosylation of Lrp4 might be involved in the pathogenesis of these CMSs. Furthermore, because Mesdc2 plays a key role in cell-surface expression of Lrp4 and MuSK-dependent postsynaptic specialization (Figs. 3 and 4C), it is tempting to speculate that mutations in *MESDC2* might be causally associated with another type of CMS with impaired NMJ formation.

Like GFPT1 and DPAGT1, Mesdc2 and Lrp4 are expressed in a wide variety of cell types. Therefore, it would be puzzling if they function only in NMJs, although NMJs are apparently susceptible to *GFPT1* or *DPAGT1* mutations. Indeed, Lrp4 plays essential roles in various developmental events including bone growth, limb patterning, and kidney formation, probably by regulating Wnt and BMP signaling [32–34]. Consistently, mutations in the *LRP4* gene were reported as a cause of Cenani–Lenz syndrome, a congenital distal limb disorder, which is sometimes accompanied by renal agenesis [33]. Also, *LRP4* mutations were reported in patients with sclerosteosis, characterized by progressive bone overgrowth [34]. Thus, it is important to investigate roles of Mesdc2 not only in NMJ formation but also in these other developmental events to understand physiological and pathophysiological roles in the Mesdc2-mediated regulation of Lrp4.

## Acknowledgements

We thank T. Kitamura for providing Plat-E cells, O. Higuchi for valuable discussion, and R. Whittier for critically reading the manuscript. This work was supported in part by grants-in-aid for scientific research (A) and scientific research on innovative areas from the Ministry of Education, Culture, Sports, Science and Technology of Japan.

## Appendix A. Supplementary data

Supplementary data associated with this article can be found, in the online version, at http://dx.doi.org/10.1016/j.febslet.2013.10.001.

## References

[1] Lin, W., Burgess, R.W., Dominguez, B., et al. (2001) Distinct roles of nerve and muscle in postsynaptic differentiation of the neuromuscular synapse. Nature 410 (6832), 1057–1064.
[2] Yang, X., Arber, S., William, C., et al. (2001) Patterning of muscle acetylcholine receptor gene expression in the absence of motor innervation. Neuron 30 (2), 399–410.
[3] DeChiara, T.M., Bowen, D.C., Valenzuela, D.M., et al. (1996) The receptor tyrosine kinase MuSK is required for neuromuscular junction formation in vivo. Cell 85 (4), 501–512.
[4] Kim, N., Stiegler, A.L., Cameron, T.O., et al. (2008) Lrp4 is a receptor for Agrin and forms a complex with MuSK. Cell 135 (2), 334–342.
[5] Zhang, B., Luo, S., Wang, Q., et al. (2008) LRP4 serves as a coreceptor of agrin. Neuron 60 (2), 285–297.
[6] Weatherbee, S.D., Anderson, K.V. and Niswander, L.A. (2006) LDL-receptor-related protein 4 is crucial for formation of the neuromuscular junction. Development 133 (24), 4993–5000.
[7] Inoue, A., Setoguchi, K., Matsubara, Y., et al. (2009) Dok-7 activates the muscle receptor kinase MuSK and shapes synapse formation. Sci. Signal. 2 (59), ra7.
[8] Wu, H., Lu, Y., Shen, C., et al. (2012) Distinct roles of muscle and motoneuron LRP4 in neuromuscular junction formation. Neuron 75 (1), 94–107.
[9] Yumoto, N., Kim, N. and Burden, S.J. (2012) Lrp4 is a retrograde signal for presynaptic differentiation at neuromuscular synapses. Nature 489 (7416), 438–442.
[10] Higuchi, O., Hamuro, J., Motomura, M., et al. (2011) Autoantibodies to low-density lipoprotein receptor-related protein 4 in myasthenia gravis. Ann. Neurol. 69 (2), 418–422.
[11] Pevzner, A., Schoser, B., Peters, K., et al. (2012) Anti-LRP4 autoantibodies in AChR- and MuSK-antibody-negative myasthenia gravis. J. Neurol. 259 (3), 427–435.
[12] Zhang, B., Tzartos, J.S., Belimezi, M., et al. (2012) Autoantibodies to lipoprotein-related protein 4 in patients with double-seronegative myasthenia gravis. Arch. Neurol. 69 (4), 445–451.
[13] Iemura, S. and Natsume, T. (). One-by-One Sample Preparation Method for Protein Network Analysis. Protein Interactions, 15, ISBN 978-953-51-0244-1, InTech, http://dx.doi.org/10.5772/37931. pp. 293–310.
[14] Honma, M., Higuchi, O., Shirakata, M., et al. (2006) Dok-3 sequesters Grb2 and inhibits the Ras-Erk pathway downstream of protein-tyrosine kinases. Genes Cells 11 (2), 143–151.
[15] Tezuka, T., Umemori, H., Akiyama, T., et al. (1999) PSD-95 promotes Fyn-mediated tyrosine phosphorylation of the N-methyl-D-aspartate receptor subunit NR2A. Proc. Natl. Acad. Sci. USA 96 (2), 435–440.
[16] Zhang, Y., Liu, R., Ni, M., et al. (2010) Cell surface relocalization of the endoplasmic reticulum chaperone and unfolded protein response regulator GRP78/BiP. J. Biol. Chem. 285 (20), 15065–15075.
[17] Tomari, T., Koshikawa, N., Uematsu, T., et al. (2009) High throughput analysis of proteins associating with a proinvasive MT1-MMP in human malignant melanoma A375 cells. Cancer Sci. 100 (7), 1284–1290.
[18] Wang, J., Fu, X.Q., Lei, W.L., et al. (2010) Nuclear factor kappaB controls acetylcholine receptor clustering at the neuromuscular junction. J. Neurosci. 30 (33), 11104–11113.
[19] Hsieh, J.C., Lee, L., Zhang, L., et al. (2003) Mesd encodes an LRP5/6 chaperone essential for specification of mouse embryonic polarity. Cell 112 (3), 355–367.
[20] Rudd, P.M., Wormald, M.R. and Dwek, R.A. (2004) Sugar-mediated ligand-receptor interactions in the immune system. Trends Biotechnol. 22 (10), 524–530.
[21] Peter-Katalinic, J. (2005) Methods in enzymology: O-glycosylation of proteins. Methods Enzymol. 405, 139–171.
[22] Moremen, K.W., Tiemeyer, M. and Nairn, A.V. (2012) Vertebrate protein glycosylation: diversity, synthesis and function. Nat. Rev. Mol. Cell Biol. 13 (7), 448–462.
[23] Liu, C.C., Pearson, C. and Bu, G. (2009) Cooperative folding and ligand-binding properties of LRP6 beta-propeller domains. J. Biol. Chem. 284 (22), 15299–15307.
[24] Bonnemaison, M.L., Eipper, B.A. and Mains, R.E. (2013) Role of adaptor proteins in secretory granule biogenesis and maturation. Front. Endocrinol. 4, 101.
[25] Belaya, K., Finlayson, S., Slater, C.R., et al. (2012) Mutations in DPAGT1 cause a limb-girdle congenital myasthenic syndrome with tubular aggregates. Am. J. Hum. Genet. 91 (1), 193–201.
[26] Fuhrer, C., Sugiyama, J.E., Taylor, R.G., et al. (1997) Association of muscle-specific kinase MuSK with the acetylcholine receptor in mammalian muscle. EMBO J. 16 (16), 4951–4960.
[27] Martin, P.T. (2003) Glycobiology of the neuromuscular junction. J. Neurocytol. 32 (5–8), 915–929.
[28] Gehle, V.M., Walcott, E.C., Nishizaki, T., et al. (1997) N-glycosylation at the conserved sites ensures the expression of properly folded functional ACh receptors. Brain Res. Mol. Brain Res. 45 (2), 215–229.
[29] Guergueltcheva, V., Muller, J.S., Dusl, M., et al. (2012) Congenital myasthenic syndrome with tubular aggregates caused by GFPT1 mutations. J. Neurol. 259 (5), 838–850.
[30] Lacazette, E., Le Calvez, S., Gajendran, N., et al. (2003) A novel pathway for MuSK to induce key genes in neuromuscular synapse formation. J. Cell Biol. 161 (4), 727–736.
[31] Moore, C., Leu, M., Muller, U., et al. (2001) Induction of multiple signaling loops by MuSK during neuromuscular synapse formation. Proc. Natl. Acad. Sci. USA 98 (25), 14655–14660.
[32] Choi, H.Y., Dieckmann, M., Herz, J., et al. (2009) Lrp4, a novel receptor for Dickkopf 1 and sclerostin, is expressed by osteoblasts and regulates bone growth and turnover in vivo. PLoS ONE 4 (11), e7930.
[33] Li, Y., Pawlik, B., Elcioglu, N., et al. (2010) LRP4 mutations alter Wnt/beta-catenin signaling and cause limb and kidney malformations in Cenani-Lenz syndrome. Am. J. Hum. Genet. 86 (5), 696–706.
[34] Leupin, O., Piters, E., Halleux, C., et al. (2011) Bone overgrowth-associated mutations in the LRP4 gene impair sclerostin facilitator function. J. Biol. Chem. 286 (22), 19489–19500.

Published September 16, 2013





# Ero1-α and PDIs constitute a hierarchical electron transfer network of endoplasmic reticulum oxidoreductases

Kazutaka Araki,[1,2] Shun-ichiro Iemura,[3] Yukiko Kamiya,[4,5] David Ron,[6,7] Koichi Kato,[4,5,8] Tohru Natsume,[1] and Kazuhiro Nagata[2]

[1]Molecular Profiling Research Center for Drug Discovery, National Institute of Advanced Industrial Science and Technology, Koto-ku, Tokyo 135-0064, Japan
[2]Laboratory of Molecular and Cellular Biology, Faculty of Life Sciences, Kyoto Sangyo University, Kita-ku, Kyoto 603-8047, Japan
[3]Innovative drug development translational research section, Fukushima Medical University, Fukushima 960-1295, Japan
[4]Institute for Molecular Science and Okazaki Institute for Integrative Bioscience, National Institutes of Natural Sciences, Okazaki 444-8787, Japan
[5]Graduate School of Pharmaceutical Sciences, Nagoya City University, Nagoya 467-8603, Japan
[6]Metabolic Research Laboratories; and [7]National Institute for Health Research Cambridge Biomedical Research Centre, Addenbrooke's Hospital; University of Cambridge, Cambridge CB2 0QQ, England, UK
[8]The Glycoscience Institute, Ochanomizu University, Tokyo 112-8610, Japan

Downloaded from jcb.rupress.org on February 18, 2014

Ero1-α and endoplasmic reticulum (ER) oxidoreductases of the protein disulfide isomerase (PDI) family promote the efficient introduction of disulfide bonds into nascent polypeptides in the ER. However, the hierarchy of electron transfer among these oxidoreductases is poorly understood. In this paper, Ero1-α–associated oxidoreductases were identified by proteomic analysis and further confirmed by surface plasmon resonance. Ero1-α and PDI were found to constitute a regulatory hub, whereby PDI induced conformational flexibility in an Ero1-α shuttle cysteine (Cys99) facilitated intramolecular electron transfer to the active site. In isolation, Ero1-α also oxidized ERp46, ERp57, and P5; however, kinetic measurements and redox equilibrium analysis revealed that PDI preferentially oxidized other oxidoreductases. PDI accepted electrons from the other oxidoreductases via its a′ domain, bypassing the a domain, which serves as the electron acceptor from reduced glutathione. These observations provide an integrated picture of the hierarchy of cooperative redox interactions among ER oxidoreductases in mammalian cells.

## Introduction

Membrane and secretory proteins are co-translationally transported into the ER and folded with the assistance of a series of chaperones, glycosylation enzymes, and oxidoreductases (Hebert and Molinari, 2007; Araki and Nagata, 2011b). Oxidoreductases in the ER ensure the efficient formation of native disulfide bonds during the folding of nascent polypeptides. The best-characterized ER oxidoreductase is protein disulfide isomerase (PDI; Freedman et al., 1994). PDI contains two thioredoxin domains, each of which contains a CXXC motif involved in dithiol–disulfide exchange reactions. PDI introduces disulfide bonds into nascent proteins as an oxidoreductase, rearranges incorrect disulfide bonds as an isomerase, and assists the folding of and prevents the aggregation of unfolded proteins as a molecular chaperone. In addition to PDI, more than 20 oxidoreductases have been identified in the mammalian ER, including ERp57, ERp44, ERp72, ERdj5, P5, and ERp46, each of which contains at least one thioredoxin-like domain (Ellgaard and Ruddock, 2005; Hatahet and Ruddock, 2009). Although some ER oxidoreductases have well-characterized specific functions (Appenzeller-Herzog and Ellgaard, 2008; Rutkevich et al., 2010; Benham, 2012), the biological implications of the diversity of ER oxidoreductases remains to be investigated.

PDI is generally thought to be the primary acceptor of oxidative equivalents from the Ero1 family of oxidases, whereas

Correspondence to Kazuhiro Nagata: nagata@cc.kyoto-su.ac.jp

Y. Kamiya's present address is Graduate School of Engineering, Nagoya University, Chikusa-ku, Nagoya 464-8603, Japan.

Abbreviations used in this paper: CBB, Coomassie brilliant blue; NEM, *N*-ethylmaleimide; NMR, nuclear magnetic resonance; PDI, protein disulfide isomerase; SPR, surface plasmon resonance; WT, wild type.

© 2013 Araki et al. This article is distributed under the terms of an Attribution–Noncommercial–Share Alike–No Mirror Sites license for the first six months after the publication date (see http://www.rupress.org/terms). After six months it is available under a Creative Commons License (Attribution–Noncommercial–Share Alike 3.0 Unported license, as described at http://creativecommons.org/licenses/by-nc-sa/3.0/).

Supplemental Material can be found at:
http://jcb.rupress.org/content/suppl/2013/09/10/jcb.201303027.DC1.html

The Rockefeller University Press $30.00
J. Cell Biol. Vol. 202 No. 6 861–874
www.jcb.org/cgi/doi/10.1083/jcb.201303027

Published September 16, 2013

the actual order of electron transfer among oxidoreductases remains to be established (Riemer et al., 2009; Araki and Inaba, 2012). Although Prx4 and vitamin K epoxide reductase were recently shown to play an auxiliary role in ER oxidative folding in mammalian cells, the Ero1 enzymes are the best-conserved ER oxidases and quantitatively dominate oxidation in the ER (Appenzeller-Herzog et al., 2010; Zito et al., 2010; van Lith et al., 2011; Araki and Inaba, 2012; Rutkevich and Williams, 2012). Recent evidence shows that PDI regulates Ero1-α activity by catalyzing the rearrangement of the regulatory cysteine pairs of Ero1-α (Araki and Inaba, 2012). Thus, PDI and Ero1-α constitute a feedback regulatory system that responds to the redox conditions of the ER (Sevier and Kaiser, 2008; Appenzeller-Herzog et al., 2010). However, the significance of the interaction of PDI with Ero1-α and role of other oxidoreductases in the disulfide transfer chain promoting efficient oxidation of nascent polypeptides in the ER needs to be further defined. Here, we present a systematic study of the kinetic interactions of Ero1-α with various ER oxidoreductases to reveal their regulatory network and molecular mechanisms.

## Results

### Ero1-α binds to ER-resident oxidoreductases

Ero1-α–interacting partners have been previously identified (see Table S1 and references therein). But here, we attempted to acquire a comprehensive dataset. FLAG-tagged Ero1-α was expressed in HEK293T cells, and the Ero1-α–associated proteins in the anti-FLAG antibody immunoprecipitates were analyzed by liquid chromatography coupled with tandem mass spectrometry (Fig. S1 A; Natsume et al., 2002). Most of the peptides recovered in complex with Ero1-α were derived from ER-resident soluble oxidoreductases, including PDI, ERp44, ERp57, ERp72, ERp46, and P5. The interactions were confirmed by immunoblotting experiments, in which immunoprecipitates from cells stably expressing FLAG-tagged Ero1-α were probed with antibodies to the oxidoreductases (Fig. 1 A). The interactions with endogenous Ero1-α were further confirmed by immunoprecipitation after transient overexpression of the tagged oxidoreductases (Fig. S1 B). Of note, active site CXXA mutants of the oxidoreductases showed the strongest interactions with Ero1-α, as demonstrated previously (Table S1; Anelli et al., 2003; Jessop et al., 2007, 2009a). Because the CXXA mutant reportedly prolongs the mixed disulfide intermediate states, these results suggest that the CXXC active sites are involved in interactions between Ero1-α and oxidoreductases (Hatahet and Ruddock, 2007; Jessop et al., 2009b).

Direct interactions of Ero1-α with the aforementioned identified oxidoreductases were assayed by surface plasmon resonance (SPR) with immobilized Ero1-α and soluble oxidoreductases under redox conditions equivalent to those in the ER: a reduced glutathione (GSH) to oxidized glutathione (GSSG) ratio of 4:1 (Fig. S1 C; Dixon et al., 2008; Araki and Nagata, 2011a). A two-state model was adopted to calculate the association and dissociation rate constants with the first equilibrium constants (Fig. S1 D). These values are shown in Fig. 1 B, in which the diagonal lines represent the dissociation constants ($K_d$). PDI clearly showed the strongest binding to Ero1-α with a $K_d$ of ~1.7 µM, which is consistent with the previously reported value (Table S1; Wang et al., 2009; Inaba et al., 2010; Araki and Nagata, 2011a; Masui et al., 2011). Ero1-α showed sequentially decreasing binding affinities to ERp44, P5, and ERp57/ERp72, and its affinity to ERp46 was the weakest. Furthermore, the binding kinetics of PDI were almost identical under different redox buffers, suggesting the interaction analyzed by SPR is independent of thiol exchange (unpublished data).

### Ero1-α oxidizes oxidoreductases in vitro

To elucidate the functional significance of these interactions of Ero1-α with other oxidoreductases, we adopted an oxygen consumption assay to monitor the oxidation by Ero1-α in the presence of GSH as the upstream electron donor, as Ero1-α transfers the pair of electrons recovered from PDI to molecular oxygen, resulting in oxygen consumption that can be monitored by an oxygen-specific electrode (Fig. 1 C; Gross et al., 2006). Oxygen consumption was not observed in the absence of an oxidoreductase (Fig. S1 E, black line), which indicates that Ero1-α inefficiently oxidizes GSH. Addition of PDI markedly stimulated oxygen consumption as previously reported (Fig. S1 E, blue line; Baker et al., 2008; Inaba et al., 2010; Araki and Nagata, 2011a).

Ero1-α activity is known to be accelerated by reduced substrate, most probably PDI, through the reduction or isomerization of regulatory disulfides (Fig. S1 F; Sevier et al., 2007; Appenzeller-Herzog et al., 2008; Tavender and Bulleid, 2010). To prevent this factor from affecting the rate of enzymatic activity, we used a constitutively active Ero1-α(C104A/C131A) (Baker et al., 2008; Araki and Nagata, 2011a). In the presence of PDI, the mutant Ero1-α consumed oxygen faster than the wild-type (WT) enzyme, as expected (Fig. S1 E, compare blue and red lines).

A similar acceleration of oxygen consumption by the constitutively active Ero1-α(C104A/C131A) was also observed upon incubation with other oxidoreductases (ERp46, ERp57, and P5), indicating that the constitutively active Ero1-α(C104A/C131A) possesses oxidase activity against these ER oxidoreductases (compare Fig. 1, D and E; Inaba et al., 2010). Interestingly, the rank order of oxygen consumption by the oxidoreductases was not perfectly correlated with their binding affinities, with the lower affinity ERp46 exhibiting higher rates of oxygen consumption than other oxidoreductases. ERp72 showed unique characteristics by exerting a negligible effect on oxygen consumption by Ero1-α, although it did physically interact with Ero1-α (Fig. 1, D and E). In summary, Ero1-α exhibited the strongest physical and catalytic interaction with PDI, which is probably caused by the sterically optimized interaction oriented by the β hairpin of Ero1-α and the hydrophobic pocket in the b′ domain of PDI (Masui et al., 2011).

### Ero1-α is dominantly regulated by PDI

Activated Ero1-α has a potential to oxidize other oxidoreductases, whereas WT Ero1-α only oxidizes PDI (Fig. 1, D and E). This result suggests that PDI could activate Ero1-α most efficiently and PDI was in turn oxidized by the activated Ero1-α. To address this point, we examined the activation of Ero1-α by the

Downloaded from jcb.rupress.org on February 18, 2014

Published September 16, 2013

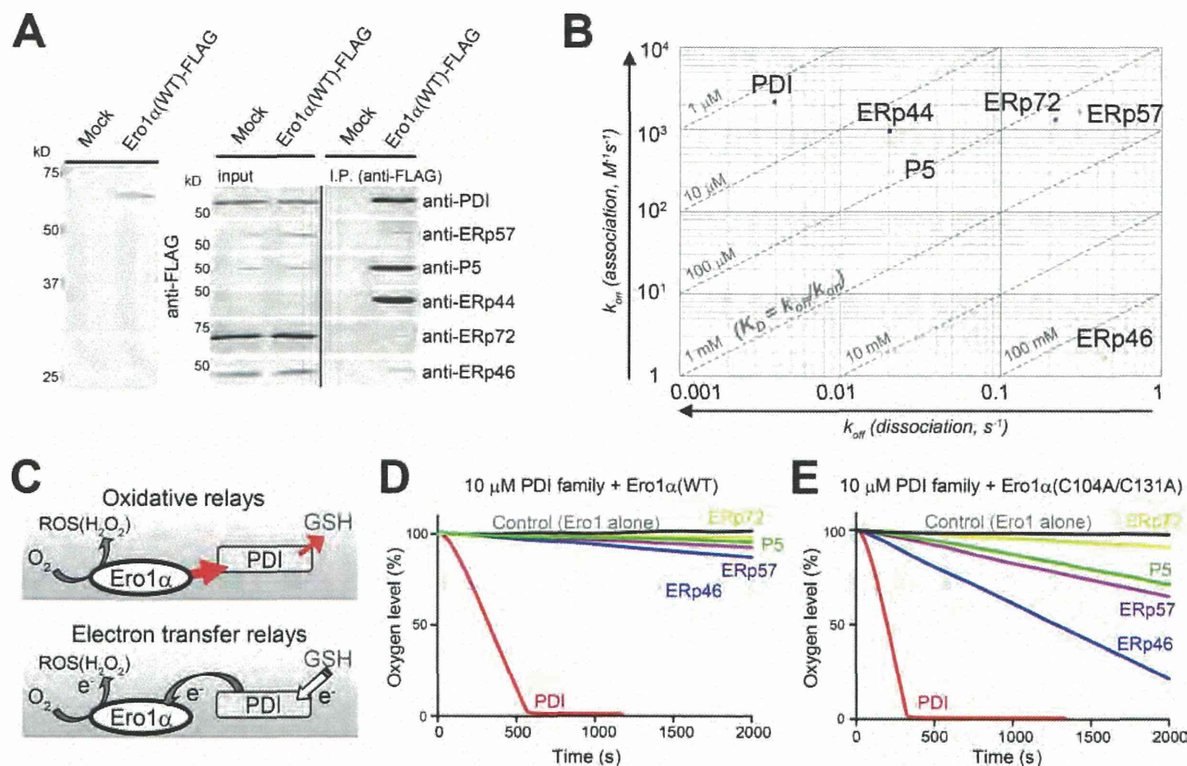


Figure 1. **Ero1-α binds to ER-resident oxidoreductases and preferentially oxidizes PDI.** (A, left) HEK293T cells (Mock) or HEK293T cells stably expressing Ero1-α–FLAG (Ero1-α(WT)–FLAG) were lysed and subjected to immunoprecipitation (I.P.) using antibodies against FLAG. (right) Resulting precipitates were examined by immunoblot analysis with the indicated antibodies. The black line on the right indicates the removal of intervening lanes for presentation purposes. (B) Association or dissociation rate constants ($k_{on}$ or $k_{off}$) were determined with a two-state reaction model, and their first equilibrium constants are plotted. Diagonal lines represent dissociation constants ($K_d$). Data represent means from at least four individual experiments (see also Fig. S1, C and D). (C) Schematic models of oxidative relays (top) and electron transfer relays (bottom) between Ero1-α and PDI. (D) Assays were conducted in a sealed chamber starting with air-saturated buffer containing 10 mM GSH, which was regarded as the 100% oxygen level (~250 μM oxygen). Control experiments are shown in Fig. S1 E. (D and E) Oxidation of reduced oxidoreductases was initiated by the injection of 2 μM Ero1-α (D) or Ero1-α(C104A/C131A) (E) and was monitored with an oxygen electrode. ROS, reactive oxygen species.

different oxidoreductases through the overexpression or knockdown of these proteins (Table S1; Appenzeller-Herzog et al., 2008). The $O_{X1}$ (active) and $O_{X2}$ (inactive) forms of endogenous Ero1-α can be separated by using nonreducing gels (Fig. S1 E; Benham et al., 2000; Appenzeller-Herzog et al., 2008). The $O_{X1}/(O_{X2} + O_{X1})$ ratio of endogenous Ero1-α was increased by the overexpression of PDI (Fig. 2 A) and decreased by siRNA-mediated PDI knockdown (Fig. 2 B and Fig. S2 A). This finding indicated that PDI could alter the activity of Ero1-α, which is consistent with a previous study (Appenzeller-Herzog et al., 2008).

Mutants of full-length PDI were created, in which the cysteines in the CXXC motif in either the a or a′ catalytic thioredoxin domains was mutated to serine (PDI(a′) or PDI(a), respectively; Fig. 2 C). Both mutants were impaired in affecting the $O_{X1}/(O_{X2} + O_{X1})$ ratio, with PDI(a) having essentially no activity, indicating that both domains of PDI contribute to the efficient activation of Ero1-α (Fig. 2 A). These observations are consistent with previous experiments, suggesting the intramolecular transfer of electrons from the a domain to the a′ domain within PDI during its oxidation by Ero1-α (Araki and Nagata, 2011a).

Overexpression or siRNA-mediated down-regulation of other oxidoreductases, including ERp57, ERp72, and ERp44, had no significant effect on the $O_{X1}/(O_{X2} + O_{X1})$ ratio (Fig. 2, A and B). Whereas the overexpression of ERp46 or P5 had a modest effect (Fig. 2 A), down-regulation of either of these oxidoreductases caused negligible changes in the $O_{X1}/(O_{X2} + O_{X1})$ ratio (Fig. 2 B). Collectively, these results demonstrate that PDI is the major regulator of Ero1-α activity, whereas other oxidoreductases contribute modestly, if at all, to such regulation.

### The flexibility of Cys99 of Ero1-α is accelerated by its interaction with PDI

To explore in further detail the Ero1-α–PDI interaction, we adopted nuclear magnetic resonance (NMR) analysis to investigate the effect of the interaction with PDI on the molecular dynamics of Ero1-α. It is technically difficult to analyze the entire three-dimensional conformation of Ero1-α by NMR because of its molecular size (~54 kD in the free form and ~110 kD in the complex with PDI). Given that cysteine residues are involved in the electron relays and their states will reflect the activity of Ero1-α, we prepared the constitutively active Ero1-α(C104A/C131A) in





Downloaded from jcb.rupress.org on February 18, 2014